Journal of Arid Environments xxx (2012) 1–8

Contents lists available at SciVerse ScienceDirect

Journal of Arid Environments

journal homepage: www.elsevier.com/locate/jaridenv

The role of vegetation and lithology in the spatial and inter-annual response of EVI to climate in drylands of Southeastern Spain

J. Cabello [a,*,1], D. Alcaraz-Segura [a,b,1], R. Ferrero [a], A.J. Castro [a], E. Liras [a]

[a] Centro Andaluz para la Evaluación y Seguimiento del Cambio Global (CAESCG), Departamento de Biología Vegetal y Ecología, Universidad de Almería, La Cañada de San Urbano, 04120 Almería, Spain

[b] Departamento de Botánica, Facultad de Ciencias, Universidad de Granada, Campus Universitario de Fuentenueva, 18071 Granada, Spain

ARTICLE INFO

Article history:
Received 14 September 2010
Received in revised form
22 November 2011
Accepted 15 December 2011
Available online xxx

Keywords:
Climate trends
Environmental controls
EVI trends
Linear mixed models
Primary production
Remote sensing
Semi-arid ecosystems
SE Iberian Peninsula

ABSTRACT

The regional spatial and inter-annual response of the Enhanced Vegetation Index (EVI, as a proxy for aboveground net primary production) to environmental controls was evaluated in drylands of SE Spain. By means of linear mixed-effects models we found that both the spatial patterns and inter-annual trends of the EVI annual mean were explained by climate variability but clearly modulated by lithology and vegetation. Along the spatial gradient, precipitation increased the EVI mean even compensating for the greater evapotranspiration of warmer sites. Limestones, with high available water content, showed the lowest dependence of EVI mean on precipitation. The greater capacity of scrublands to store and use soil moisture was only evident on marls sites. The observed 2001–2010 trends toward less stressful conditions (precipitation rises and temperature declines) led to EVI mean increases. This EVI mean response was steeper in grasslands, with shallow roots, and marls, with low available water content. The study revealed the importance of analyzing the seasonal timing of trends in Mediterranean drylands, where temperature and precipitation are out of phase. The observed earlier rain-arrival after summer drought and cooler early-autumn, caused very strong EVI increases at the beginning of the growing season that may favor the rest of the season.

1. Introduction

Drylands of the Mediterranean basin, where precipitation and temperature are out of phase, are particularly sensitive to the intensification of aridity conditions (Giorgi and Lionello, 2008). The response of aboveground net primary production (ANPP) to precipitation represents an effective and straightforward approach to evaluate drylands status and trends (Verón et al., 2006). However, there exist differences between the spatial and temporal models that relate ANPP to climate factors (e.g. Jobbagy et al., 2002; Le Houérou et al., 1988), suggesting that other biotic and abiotic factors are involved.

In addition to precipitation, abiotic controls include temperature, land-surface and soil properties, and topography. Temperature has both a direct and indirect effect on ANPP. In energy-limited environments, cold temperatures constrain ANPP and determine the seasonality and starting date of the growing season (e.g. Jobbagy et al., 2002). In water-limited environments, temperature increases potential evapotranspiration, which may constrain ANPP (Le Houérou, 1990). Soil structure, texture, depth, and chemical composition control the soil water holding capacity (Russell and Wild, 1988), which is particularly important for determining the partition of annual precipitation use between wet and dry seasons (Le Houérou, 1984). Topography and solar irradiation also influence water redistribution and ANPP (Jobbagy et al., 2002). In addition, soil biogeochemical constraints, such as soil N content, can limit both ANPP (Epstein et al., 2005) and rain use efficiency (Bai et al., 2008). Land-surface biogeophysical properties such as albedo or surface temperature also affect evapotranspiration and ANPP (García et al., 2008).

Another fraction of the ANPP variance relates to biotic features of ecosystems (Huxman et al., 2004; Webb et al., 1983). Functional and structural traits of vegetation, such as canopy type, species diversity, or root depth, determine water use efficiency and, hence, ANPP at the regional scale. Species diversity increases the probability of including different plant functional types and a broader range of strategies to gain resource use efficiency (Chapin et al., 1997). Lloret et al. (2007) showed how the impact of dramatic water shortage on vegetation greenness depends on the presence of species able to cope with drier conditions. In arid SE Spain,

* Corresponding author. Tel.: +34 950 015932; fax: +34 950 015069.
E-mail address: jcabello@ual.es (J. Cabello).
[1] Both authors contributed equally to this work.

0140-1963/$ – see front matter © 2011 Elsevier Ltd. All rights reserved.
doi:10.1016/j.jaridenv.2011.12.006

Miranda et al. (2009a) also found high resistance in the response of annual plant communities to reductions in water supply thanks to the presence of species adapted to high climate variability. Plant spatial distribution also affects water use efficiency and productivity in this area, being higher when *Stipa tenacissima* L. tussocks are perpendicularly distributed to the maximum slope (Puigdefábregas et al., 1999). In the Patagonian steppe, plant density has also been shown to be a control of ANPP recovery after drought (Yahdjian and Sala, 2006). Root depth, size, shape, distribution, and competition are very important in water-limited environments, since they determine the amount of soil explored to take up water and nutrients (Schenk and Jackson, 2002). For example, shrubs generally have deeper roots than grasses, which allow shrubs to explore larger volumes of soil and, hence, to better buffer the inter-seasonal and inter-annual variability in precipitation (Haase et al., 2000).

Two critical limitations for the study of the environmental controls of ANPP across space and time are the difficulty in obtaining repeated regional estimates of ANNP and the lack of long-enough time-series (Fabricante et al., 2009; Knapp and Smith, 2001). Remote sensing tools help to overcome both limitations (Alcaraz-Segura et al., 2009a). First, spectral vegetation indices of vegetation greenness (such as the Normalized Difference Vegetation Index – NDVI – , or the Enhanced Vegetation Index –EVI –) can be used to estimate ANPP at the regional scale through the operative and conceptually solid model of Monteith (1972). Vegetation indices are commonly used to estimate leaf area index, the fraction of photosynthetically active radiation absorbed by the canopy (fAPAR) (Sellers et al., 1992), and ANPP (e.g. Paruelo et al., 2000; Piñeiro et al., 2006). Second, since different satellites have been repeatedly capturing this kind of spectral information during the past few decades, they provide a collection of long-enough time-series of satellite images, which currently constitute our best tool to track ANPP at the regional scale (Pettorelli et al., 2005).

Spectral vegetation indices have been extensively used in the study of semi-arid ecosystems in SE Spain. Many of these studies focused on the evaluation of drylands condition and degradation (e.g. Boer and Puigdefábregas, 2003; Camacho-De Coca et al., 2004; García et al., 2008; Liu et al., 2004), and the estimation of evapotranspiration and recharge (Contreras et al., 2008; García et al., 2008). However, few studies have taken advantage of vegetation indices as proxies or estimators of ANPP (Miranda et al., 2009a), absorbed photosynthetically active radiation (APAR) (Oyarzabal et al., 2008; Oyonarte et al., 2010; Paruelo et al., 2005), or leaf area index (Serrano-Ortiz et al., 2007). From these, only two works have formally evaluated the response to precipitation of NDVI-derived surrogates of ANPP in drylands of SE Spain at the local (Miranda et al., 2009a) and regional (Paruelo et al., 2005) scales. Miranda et al. (2009a) used NDVI to evaluate the response of ANPP to controlled precipitation reductions in annual plant communities. Paruelo et al. (2005) used NDVI to evaluate the differences in the APAR-precipitation correlation between protected and non-protected landscapes.

In this article, our aim was to evaluate, by means of linear mixed models, the regional spatial and inter-annual response of the Enhanced Vegetation Index (our proxy for ANPP) to both precipitation and temperature, but also accounting for the role of vegetation and lithological substrate and their interactions. The following hypotheses guided our study:

- Since drylands of SE Spain are water-limited environments, precipitation should be the main control of EVI. In addition, temperature should also play an important role since it increases potential evapotranspiration and water stress in drylands (Haase et al., 1999; Le Houérou, 1990), hence reducing EVI.
- Dominant plant species of drylands of SE Spain are known to differ in their strategies for water control. For example, due to their deeper roots and less dense canopies, shrubs of *Anthyllis cytisoides* L. and *Retama sphaerocarpa* (L.) Boiss. showed lower rainfall interception, lower direct canopy evaporation rates, higher stemflow, and, hence, higher percolation of rainfall to deeper soil layers than the tussock grass of *S. tenacissima* (Domingo et al., 1998). Hence, shrubs would increase deep-soil water storage and use, and improve hydraulic lift (e.g. Prieto et al., 2010), while the shallow-rooted *S. tenacissima*, adapted to use sporadic rainfall pulses (Haase et al., 1999), would depend on soil moisture from top layers. We hypothesized that EVI in grasslands would be lower than in scrublands as a result of greater sensitivity to water stress and higher dependence on annual rainfall.
- Differences in lithology may also affect EVI since substrates differ in soil water retention and land-surface physical properties. Soil water content in the macro-pores (known to be easily lost by gravity) is known to be the most valuable predictor for estimating leaf growth in individuals of *S. tenacissima* (Haase et al., 1999). Cabello (1997) showed higher soil available water capacity on limestones than on marls, phyllites and schists as a result of their textural differences (Table 1). García et al. (2008) also pointed out that the former substrates differed in their energy partitioning between latent and sensible heat, inducing differences in vegetation transpiration. These controls of lithology on the water dynamics suggest the existence of a strong effect of lithology on the EVI.

2. Methodology

2.1. Study area

The study area was restricted to drylands of Andalusia in Southeastern Spain (36°46′ N, 1°40′ W to 37°29′ N, 3°07′ W) (Fig. 1). The analysis was focused on the most representative vegetation types of the region: scrublands and perennial grasslands (alpha steppes). Scrublands are dominated by chamaephytes adapted to dry and semi-arid conditions (Cabello, 2009), such as *A. cytisoides*, *Anthyllis terniflora* (Lag.) Pau, *Cistus* spp., *Genista umbellata* (L'Hér.) Dum, *Helianthemum almeriense* Pau, *Phlomis purpurea* L., *R. sphaerocarpa*, *Rosmarinus officinalis* L., *Sideritis* spp., *Teucrium* spp., *Thymus* spp. and *Ulex parviflorus* Pourr.. Perennial grasslands are alpha steppes largely dominated by the perennial tussock grass *S. tenacissima*. Both vegetation types are representative of drylands of the Western Mediterranean Region.

2.2. Datasets and pixel selection

From the different spectral vegetation indices available, we chose the Enhanced Vegetation Index (EVI) as a surrogate of ANPP since it is more resistant to both soil influences and atmospheric effects than NDVI. EVI was introduced by Huete et al. (1997) by

Table 1
Soil texture and moisture description of 21 sites distributed across the study area (for details see Cabello, 1997). Mean and standard deviation for percentage of clay and sand, Available Water Content (AWC in mm) and Water Holding Capacity (WHC in mm).

	% Clay	% Sand	AWC	WHC
Limestones	17.6 ± 8.4	52.2 ± 15.2	1.0 ± 0.4	32.8 ± 16.1
Marls	10.8 ± 3.2	63.5 ± 17.2	0.7 ± 0.4	11.3 ± 7.0
Phyllites & Schists	9.5 ± 5.1	66.9 ± 11.0	0.9 ± 0.4	16.1 ± 8.9

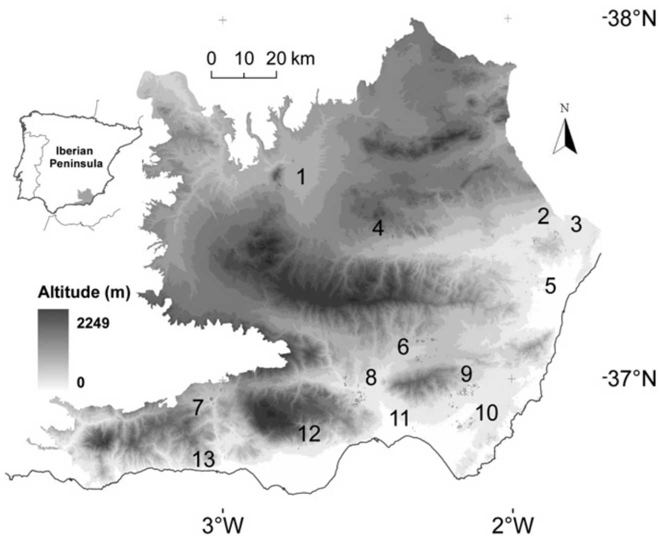

Fig. 1. Study area. Drylands of Andalusia in SE Spain. Black dots show 137 pure 230 × 230 m MODIS pixels were sampled within a 5-km buffer and 100-m altitudinal range around 13 meteorological stations with data available online: 1) Baza, 2) Huercal–Overa, 3) Cuevas de Almazora, 4) Tíjola, 5) Antas, 6) Tabernas, 7) Ugíjar, 8) Alhama, 9) Níjar, 10) San Isidro, 11) Almería, 12) La Mojonera, and 13) Adra (RIA Network: www.juntadeandalucia.es/agriculturaypesca/ifapa/ria, RAIF Network: http://dgpa.besana.es/clima/inicio.do).

taking advantage of two former improvements made to NDVI: the Soil-Adjusted Vegetation Index (SAVI) (Huete, 1988) and the Atmospherically Resistant Vegetation Index (ARVI) (Kaufman and Sendra, 1988; Kaufman and Tanre, 1992, 1996). On the one hand, SAVI adds and adjustment factor "L" into NDVI to compare canopies with dark and light soil backgrounds. Normally "L" is set to 0.5, but for low vegetation cover such as drylands, "L" can be set to 1. On the other hand, ARVI incorporates a self-correction process into NDVI that automatically corrects the atmospheric effect in the red band by introducing the blue band into the NDVI formulas. As a result, compared to NDVI, EVI is more sensitive to changes in areas having high biomass (a serious shortcoming of NDVI), reduces the influence of atmospheric conditions on vegetation index values, and corrects for soil background signals.

Our study was based on a time-series of EVI satellite images provided by the MODIS (Moderate Resolution Imaging Spectrorradiometer) Terra sensor from January 2001 to December 2010. We used MOD13Q1 product, which provides 23 EVI maximum value composite (MVC) images per year (every sixteen days) with an approximated pixel size of 230 × 230 m. The images are geometrically and atmospherically corrected and include quality assessment flags that we used to mask those pixels flagged as cloud, shade, water, snow, and with high aerosol content. For each year, we calculated the EVI annual mean and obtained the long-term average of the EVI annual mean (EVI_mean) as a surrogate of average ANPP.

The selection of pixels was carried out in four steps. First, we only used pixels within a 5-km buffer and within an altitude range of 100 m around 13 meteorological stations (RAIF and SIVA Networks, Fig. 1). Then, we used the vegetation map of Andalusia (scale: 1:10,000, years: 1996–2006) and the land-use information system of Spain (SIOSE2005 for Andalusia, scale: 1:10,000, years: 2004–2006) to select only those pure pixels at the both maps that corresponded to scrublands and alpha steppes. For each pure pixel, we identified the dominant (>90%) lithological substrate according to the lithological map of Andalusia (scale: 1:50,000, year: 2004, Spanish Institute for Geology and Mining). Finally, we used orthophotos of Andalusia (pixel size: 0.5 m, year: 2008) to visually double check the final selection of 337 pixels (Fig. 1). All datasets can be downloaded from the official website of the Environmental Information Network of Andalusia (REDIAM, http://www.juntadeandalucia.es/medioambiente/site/rediam). Scrublands ($n = 134$) and grasslands ($n = 203$) samples were distributed across all meteorological stations and lithological substrates (pixel percentages for scrublands: clays and silts = 5, conglomerates = 37, limestones = 27, marls = 8, phyllites and schists = 7, and sandstones = 15; for grasslands: clays and silts = 18, conglomerates = 28, limestones = 20, marls = 13, phyllites and schists = 9, and sandstones = 12).

Since climatic data for the first half of 2001 were not available in Níjar station, we used forward stepwise regressions to estimate the missing data. Variables were mean annual temperature, total annual precipitation, and the mean temperatures and accumulated precipitations of the MODIS 16-day MVC periods in Níjar (dependent variables) and in the remaining stations (independent variables) from 2002 to 2010. Akaike Information Criterion (AIC) and Bayesian Information Criterion (BIC) were used as a trade-off between significance and simplicity to select the final equations used to fill Níjar gaps.

2.3. Data analysis

We built two Linear Mixed Models (LMMs) using the nlme (Piñeiro et al., 2009) and lme4 (Bates and Sarkar, 2007) R packages. LMMs are particularly useful to account for nested sampling designs (Bolker et al., 2009), where the autocorrelation of samples (pixels) within sites (meteorological stations) is accounted for through the introduction of random effects. We followed the steps suggested by Zuur et al. (2009) as a procedure to build the two models. First, using the full model for the fixed effects, we found the optimal structure for the random component using restricted maximum likelihood (REML). Then, to find the optimal fixed structure, the trade-off between significance and simplicity was evaluated by iteratively comparing more complex models to simpler models and choosing the one with lower AIC and BIC, and significant χ^2 test for the Log-likelihood (using maximum likelihood and always maintaining the same random structure). We present the final model using REML and checked for the absence of significant correlation among independent variables and for normality of residuals. To assess the overall goodness of fit we provide the correlation between the fitted and the observed values (Bogner et al., 2010). We also calculated Edwards' R^2 statistic (Edwards et al., 2008) for the fixed effects, which compares the full model with a null model with all fixed effects deleted (except typically the intercept) while retaining exactly the same covariance structure. Though it is conceptually different to the partial R^2 in linear regression, this statistic can be similarly interpreted in the sense that it measures the marginal improvement or reduction in unexplained variability in the fixed component after accounting for a given predictor effect.

The first model evaluated the environmental controls of the spatial patterns of EVI_mean (Table 2). Fixed effects (factors whose effects at each level we were interested in) included: vegetation type, lithological substrate, mean annual precipitation (MAP), mean annual temperature (MAT), and their first order interactions. The meteorological station was considered a random effect, i.e. a factor where the interest lies in the variation among them rather than specific effects of each site. MAP and MAT were centered around their mean values to avoid correlation between them and the fixed intercept (as suggested by Zuur et al., 2009).

The second model evaluated the environmental drivers of the inter-annual trends of EVI_mean (Table 3). First, we calculated the

Table 2
Linear mixed model results for the evaluation of the environmental controls of the spatial pattern of the EVI_mean (a proxy of primary production) in drylands of SE Spain. Fixed effects were mean annual temperature (MAT), mean annual precipitation (MAP), vegetation type, lithology, and their interactions. The random effect was the meteorological station. Analysis based on normal errors and AIC using ML estimation, with EVI_mean between 0 and 1, and MAT and MAP centered. Significance threshold was p-value < 0.05. $\text{EVI\_mean} = \alpha + \beta_1\text{MAP*MAT} + \beta_2\text{MAP*Litho} + \beta_3\text{Veget*Litho} + \beta_4\text{Litho} + b_i^{a} + \varepsilon_{ij}^{b}$.

Fixed effects (Partial R^2)	Class		Estimate β ($\times 10^4$)	SE ($\times 10^4$)	df	t	p-value
MAP*MAT (0.21)			0.9	0.4	11	2.019	0.069
MAP*Lithology (0.15)	Clays & silts		1.2	1.2	307	1.004	0.316
	Limestones		0.0	1.0	307	0.004	0.997
	Conglomerates		1.7	0.7	307	2.300	*0.022
	Marls		2.9	1.1	307	2.778	**0.006
	Phyllites & schists		2.5	0.9	307	2.861	**0.005
	Sandstones		4.2	1.1	307	3.777	***0.000
Vegetation*Lithology (0.14)	Ref. (Grasslands)						
	Scrublands	Clays & silts	−50.3	48.6	307	−1.035	0.302
		Limestones	−30.0	32.1	307	−0.937	0.350
		Conglomerates	3.9	27.6	307	0.142	0.887
		Marls	260.6	46.1	307	5.659	***0.000
		Phyllites & schists	50.7	52.5	307	0.966	0.335
		Sandstones	21.5	41.3	307	0.520	0.604
Lithology (0.06)	Ref. (Clays & silts)						
	Limestones		103.1	44.2	307	2.331	*0.020
	Conglomerates		−6.4	39.0	307	−0.164	0.870
	Marls		−151.1	47.2	307	−3.201	**0.002
	Phyllites & schists		56.0	52.3	307	1.071	0.285
	Sandstones		39.1	45.8	307	0.853	0.394
Intercept α			1506.8	42.4	307	35.568	***0.000

Goodness of fit (Pinheiro) = 0.474, Edwards' R^2 for the fixed effects = 0.224.
[a] Random effects (b_i): Meteorological station with intercept mean = 0 and variance = $0.537*10^{-4}$.
[b] Model error (ε_{ij}): mean = 0 and variance = $1.564*10^{-4}$.

slope and significance of the 2001–2010 trends for EVI_mean, MAP, and MAT. To minimize the influence of errors, outliers, missing data, and serial dependence on the slope estimations (Gilbert, 1987), we used a non-parametric linear slope estimator suggested by Sen (1968). Sen's Method for the slope calculates the median of all possible two-point slopes between pairs of years (Hirsch et al., 1982) but discards tied observations (Hollander and Wolfe, 1973). The Mann–Kendall trend test was used to evaluate the significance of the trend, since it is a rank-based test robust against non-normality, heteroscedasticity, and missing values

Table 3
Linear mixed model results for the analysis of the environmental drivers of the inter-annual 2001–2009 trends of the EVI_mean (a proxy of primary production) in drylands of SE Spain. Fixed effects were trends in mean annual temperature (MAT_trends), trends in mean annual precipitation (MAP_trends), vegetation type, lithology, and their interactions. The random effect was the meteorological station. Analysis based on normal errors and AIC using ML estimation. Significance threshold was p-value < 0.05. $\text{EVI\_mean trends} = \beta_1\text{MAT\_trends*Litho} + \beta_2\text{MAP\_trends*Litho} + \beta_3\text{Veget} + \beta_4\text{Litho} + b_i^{a} + \varepsilon_{ij}^{b}$.

Fixed effects (Partial R^2)	Class		Estimate β ($\times 10^{-4}$)	SE ($\times 10^{-4}$)	df	t	p-value
MAT_trends*Lithology (0.17)	Clays & silts		−532.1	143.2	301	−3.717	***0.000
	Limestones		−349.3	121.3	301	−2.880	**0.004
	Conglomerates		−296.9	99.7	301	−2.978	**0.003
	Marls		−285.9	150.6	301	−1.898	0.059
	Phyllites & schists		−174.6	113.7	301	−1.536	0.126
	Sandstones		−177.0	147.9	301	−1.197	0.232
MAP_trends*Lithology (0.16)	Clays & silts		−0.1	0.3	301	−0.295	0.768
	Limestones		−0.4	0.2	301	−2.273	*0.024
	Conglomerates		−0.2	0.2	301	−1.485	0.139
	Marls		−0.8	0.2	301	−3.528	**0.001
	Phyllites & schists		−0.3	0.2	301	−1.820	0.070
	Sandstones		−0.3	0.3	301	−1.157	0.248
Vegetation (0.23)	Grasslands		−13.1	16.4	301	−0.799	0.425
	Scrublands		−33.3	16.2	301	−2.048	*0.042
Vegetation*Lithology (0.18)	Ref. (Grasslands: Clays & silts)						
	Scrublands	Limestones	22.8	5.8	301	3.962	***0.000
		Conglomerates	18.6	5.5	301	3.371	**0.001
		Marls	16.8	6.6	301	2.558	*0.011
		Phyllites & schists	25.8	7.3	301	3.559	***0.000
		Sandstones**	17.8	6.3	301	2.823	**0.005
Lithology (0.23)	Ref. (Clays & silts)						
	Limestones		12.6	19.2	301	0.657	0.512
	Conglomerates		20.0	14.6	301	1.371	0.172
	Marls		36.6	16.9	301	2.167	*0.031
	Phyllites & schists		30.9	16.9	301	1.823	0.069
	Sandstones		35.0	19.4	301	1.801	0.073

Goodness of fit (Pinheiro) = 0.652, Edwards' R^2 for the fixed effects = 0.2299.
*, $p < 0,05$.
**, $p < 0,01$.
***, $p < 0,001$.
[a] Random effects (b_i): Meteorological station with intercept mean = 0 and variance = $165.21*10^{-4}$.
[b] Model error (ε_{ij}): mean = 0 and variance = $148.13*10^{-4}$.

(Alcaraz-Segura et al., 2009b, 2010). However, only 50% of pixels simultaneously exhibited significant trends (p-value < 0.01) for EVI_mean, MAP, and MAT, so we eventually decided to include all Sen's slopes in the LMM analysis regardless of their significance. Both tests were run using the Mann–Kendall package available through the MATLAB Central file exchange (http://www.mathworks.com, accessed September 2009). Second, to build the LMM we considered the slope of EVI_mean trends as the dependent variable. Independent variables were the trends in MAP, the trends in MAT, vegetation type, lithological substrate, and their first order interactions as fixed effects; and meteorological stations as random effects.

3. Results

3.1. Controls of the spatial patterns of EVI_mean

The first LMM, explaining the spatial patterns of EVI_mean (Table 2), included an intercept of 0.15 for the fixed effects that represents the basal EVI_mean under average climate conditions (average MAP and MAT of the region, since the variables were centered around their mean values). The model also retained the effect of the interactions MAP*MAT, MAP*Lithology, Vegetation*Lithology, and the main effect of Lithology (AIC = −1951.528, BIC = −1871.306, Log-likelihood = 996.764), with normal distribution of the random intercept (meteorological station, with mean = 0, variance = $0.537*10^{-4}$) and the error term (mean = 0, variance = $1.564*10^{-4}$). The overall model goodness of fit was 0.474 and Edwards' R^2 for the fixed effects was 0.224. Correlation among observations within the same site was low (0.26) but significant. MAP had a positive effect on EVI_mean through its interaction with MAT and lithology (Table 2). In the case of MAT, the positive interaction with MAP was weak and barely significant (p-value = 0.069, t = 2.019, df = 11). Even though, we included it in the model since this is a reasonable interaction that showed the greatest partial R^2 (0.21) and INS> its removal decreased the model performance (higher AIC = −1948.600 and a significant likelihood ratio = 4.93, p-value = 0.026, df = 1). The EVI_mean response to precipitation varied among lithological substrates (Table 2). The EVI_mean dependence on MAP was the highest in sandstones, followed by marls, phyllites and schists, and conglomerates. Contrary, the annual EVI_mean in areas with limestones, and clays and silts seemed to be less dependent on annual rainfall. EVI_mean only differed between vegetation types in particular lithological substrates. Scrublands significantly showed much greater EVI_mean than grasslands when growing on marls (Table 2). Lithology itself resulted in a significant control of the EVI_mean spatial pattern (Table 2). EVI_mean was significantly higher on limestones while significantly lower on marls than on the remaining lithological substrates.

3.2. Drivers of the EVI_mean inter-annual trends

Most sampled pixels showed positive EVI_mean trends (87%), positive MAP trends (100%), and negative MAT trends (95%). The second LMM, explaining the drivers of EVI_mean trends (Table 3), did not include any basal intercept for the fixed effects and retained the effect of the interactions MAT_trends*Lithology, MAP_trends*Lithology, and Vegetation*Lithology, and the main effects of Vegetation and Lithology (AIC = 2600.905, BIC = 2698.307, LogLik = −1274.453), with normal distribution for the random effects intercept (mean = 0, variance = $165.21*10^{-4}$) and for the error term (mean = 0, variance = $148.13*10^{-4}$).The overall model goodness of fit was 0.652 and Edwards' R^2 for the fixed effects was 0.230. Correlation among observations within the same site was 0.53. Inter-annual trends of the EVI_mean were significantly related to the inter-annual rises in annual accumulated precipitation (MAP_trends) through its interaction with lithology (Table 3). Only the EVI_mean increases on marls and limestones were significantly lower with MAP rises, but not on the remaining substrates. EVI_mean increased significantly more with declines in MAT on particular substrates. The greatest EVI_mean increases related to MAT declines occurred on clays and silts, followed by limestones, and conglomerates (marls almost significantly showed the same effect). MAT declines were not significantly related to EVI_mean increases on sandstones and phyllites (Table 3). The EVI_mean trends also differed among vegetation types. Grasslands significantly tended to show higher EVI_mean trends than scrublands, particularly on clays and silts. Lithology played an important role in determining the EVI_mean inter-annual trends. In addition to the interactions between lithological substrates and vegetation and climatic factors trends, the EVI_mean inter-annual positive trends were significantly greater on marls (and almost significantly on sandstones and phyllites and schists) than in the remaining substrates (Table 3). Vegetation type and lithology showed the highest partial R^2 (0.23 in both cases, Table 3).

4. Discussion

4.1. EVI_mean response to climate factors

Mean annual precipitation (MAP) and mean annual temperature (MAT), both with a relatively narrow range across meteorological stations (210–368 mm, and 15–19 °C, respectively) were not included as main effects to explain the spatial patterns of EVI_mean (Table 2). Even though, the interaction between them and with lithology revealed the clear effect of climate on drylands primary production. The positive interaction between MAP and MAT (highest partial R^2, Table 2) in the first LMM revealed that, on average, wetter sites that were simultaneously warmer, were also greener. In wetter sites, greater inputs of rainfall may compensate for the higher temperatures and subsequent greater evapotranspiration rates. In addition, MAP also raised EVI_mean through its positive interaction with lithology, which reinforces the role of precipitation as an important control of EVI in drylands (Table 2).

Trends in MAP and MAT were also not included as main effects in the second model to explain inter-annual trends of EVI_mean (Table 3). However, the interaction between MAT trends and lithology revealed how the observed general declines in temperature (Fig. 3) resulted in EVI_mean increases in most lithologies (Table 3). Such an important effect of declines in temperature agrees with the predictions that arid regions are particularly sensitive to temperature due to its effect on vegetation water demands (Haase et al., 1999; Le Houérou, 1990).

Several studies have shown the important effects of the seasonal timing of rainfall on primary production, evapotranspiration, and rainfall use efficiency (e.g. Fang et al., 2005; Porporato et al., 2002; Potts et al., 2006). The fact that the EVI_mean increases tended to be lower with greater rises of MAP in a few substrates, would contradictorily suggest that precipitation rises do not favor EVI increases in drylands. Fig. 3 reveals the importance of taking into account the seasonal timing of the rainfall trends to understand their effect in the EVI trends. A particular increase in the amount of cumulated annual precipitation would cause a more dramatic increase on EVI if precipitation increases occur during water-deficit periods, than if they occur during water-surplus periods. This is the case in our study area (Fig. 3). The analysis of the seasonal timing of the inter-annual trends in EVI, temperature, and precipitation revealed that the earlier arrival of the first rains after summer drought (displacement of rainfall from mid-autumn to late-summer) and the cooler temperatures during late-summer/early-autumn caused very strong

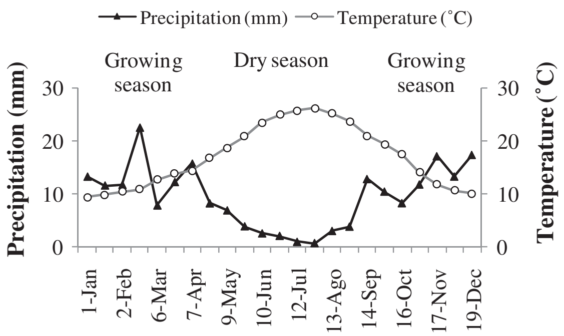

Fig. 2. Climate diagram of the sampled drylands of Andalusia in SE Spain for the 2001–2010 period. The seasonal dynamics of temperature and precipitation (being out of phase) determines a growing season from early-autumn to late spring and a non-growing season during the summer drought.

increases in EVI at the beginning of the growing season (mid-autumn) (Fig. 3). An earlier and greener (more vigorous) recovery from summer drought stress may facilitate EVI increases that occur during the middle of the growing season (from late-winter to mid-spring). However, the strong precipitation increases observed in December and January did not have an immediate effect on mid-winter EVI (constrained by the low winter temperatures, Fig. 2) but probably led to the observed increases of spring EVI, compensating for the observed reduction of spring precipitation (Fig. 3). This important effect of the timing of autumn rainfalls on primary production was also suggested in a one-season greenhouse experiment by Miranda et al. (2009b). Using pots filled with soils from Tabernas desert, these authors observed a decay of primary production of seedlings due to manipulated delays in the onset of autumn rainfalls.

4.2. Vegetation types as biotic control of EVI

Differences in vegetation structure between scrublands and grasslands explained part of the variation in the spatial pattern and inter-annual trends of EVI_mean. Vegetation types differed in their EVI_mean through their interaction with lithology (Table 2). Scrublands growing on marls showed significantly higher EVI_mean than grasslands. Marls, showing the lowest EVI_mean, were probably the most water-limiting substrate (Table 1) (Cabello, 1997; García et al., 2008). On marls, the greater diversity of plant functional types of scrublands, including shallow-rooted (e.g. therophytes and grasses) and deeper-rooted species (e.g. perennial and deciduous shrubs), capitalizes on both weak and strong precipitation events respectively (Yahdjian and Sala, 2006). Grasslands, with lower capacity to store and use water from the deeper soil (Domingo et al., 1998) would be more dependent on the recurrence of rainfall events (Haase et al., 1999). The inter-annual EVI_mean trends also showed this steeper dependence on annual rainfall of grasslands (particularly on clays and silts, and marls compared to scrubland) (Table 3) in response to the observed precipitation rises and temperature declines of the region (Fig. 3). Scrublands, on the contrary, showed higher inertia in the EVI response to the observed climate trends. In a previous work, Liras (2010) showed how more woody communities displayed weaker EVI increases with precipitation rises than less woody communities (across grasslands, scrublands, bushlands, and woodlands).

4.3. Lithology as abiotic control of EVI

Lithology modulated both the effect of MAP on the spatial patterns of EVI_mean, and the EVI_mean response to inter-annual trends in temperature and precipitation. Many works have shown how soil properties, particularly water holding capacity, can be the main drivers of drylands productivity (e.g. Epstein et al., 2005; Le Houérou et al., 1988). In the first LMM, along the spatial gradient (Table 2), pixels on marls showed lower than average EVI_mean values but a significant high dependence on MAP. On the contrary, pixels on limestones showed the highest EVI_mean values but not a significant dependence on MAP. In natural sites of a nearby region, García et al. (2008) showed how the lower available water content of marls compared to limestones implied a higher

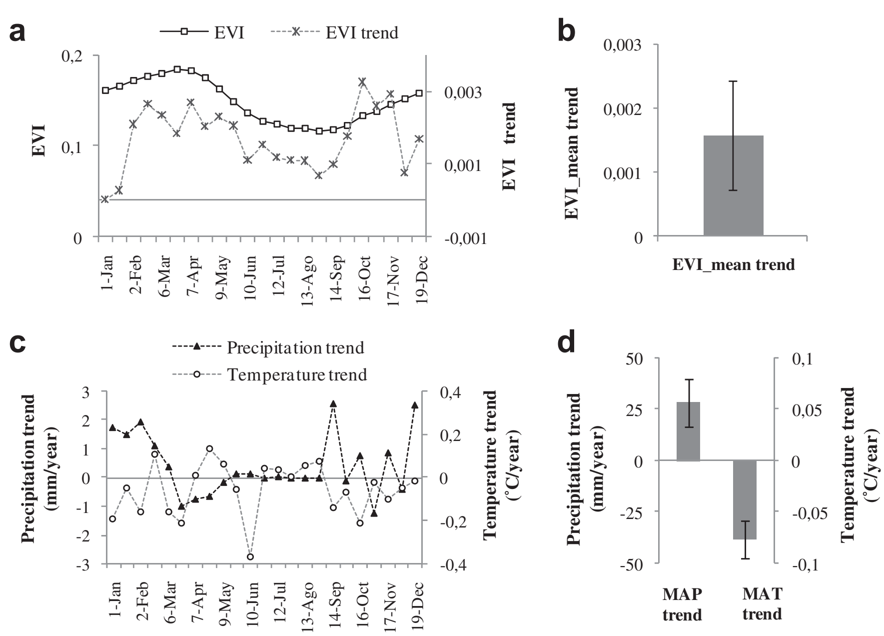

Fig. 3. Inter-annual trends along the 2001–2010 study period for a) the seasonal EVI values (the mean seasonal EVI curve is also shown), b) the EVI annual mean (EVI_mean, a surrogate of primary production), c) seasonal temperature and precipitation values, and d) mean annual temperature (MAT) and mean annual precipitation (MAP) values. *Y* axes represent the average Sen's slope of 137 sampled pixels.

sensitivity of marls vegetation greenness to summer drought. In addition to limestones, vegetation greenness on clays and silts (with the finest textures, Table 1) did not show significant dependence on MAP. Contrary, vegetation growing on sandstones, with a very coarse soil texture, showed the greatest dependence on MAP, but not a significantly greater EVI_mean than the rest of the substrates (Table 2). At a first glance, these results seem to contradict the inverse-texture hypothesis (Noy-Meir, 1973), which states that drylands ANPP should be higher on coarse-texture than on fine-texture soils. The argument is that in xeric ecosystems, fine-textured soils may favor water losses through evaporation of the water stored in the top layer (Noy-Meir, 1973), which would partially offset greater water holding capacity (Knapp et al., 2008). This hypothesis has been broadly supported across different regions with cold, dry winters and warm, wet summers (e.g. Austin and Sala, 2002; Lane et al., 1998; Sala et al., 1988). However, we speculate that in Mediterranean semi-arid areas (where temperature and precipitation are out of phase, Fig. 2), the absence of rainfall during the summer would not cause such important water losses through evaporation from fine-texture soils as in wet summer climates. Contrary, the greater water holding capacity of finer soils could offer greater water availability after summer drought to start a new growing season (Porporato et al., 2002). This agrees with the observed greater annual EVI_mean values and lower dependence on MAP in limestones, and clays and silts than in phyllites and schists, and marls (Table 2).

In the second LMM (Table 3), pixels on marls showed the highest inter-annual EVI_mean increases. Other coarse-texture substrates, such as sandstones, and phyllites and schists also showed high and nearly significant EVI_mean increases. To interpret the effect on the EVI trends of the interaction of lithology with MAP trends, it would be necessary to formally account for the seasonal timing of the rainfall trends as stated above (Fig. 3). The effect that lithology had on the positive response of EVI_mean to long-term temperature declines, could be related to substrates texture. In addition to the reduction of transpiration, temperature decreases would be particularly beneficial in fine-textured substrates since, as formerly explained, they tend to suffer greater water losses through top-layer evaporation than coarse-textured substrates (Noy-Meir, 1973). This potential benefit of fine-textured substrates (e.g. clays and silts, limestones, and conglomerates), which is more important under hot and sunny weather, might be occurring during the warmer parts of the growing season in our study area (i.e. May, June, September, and October).

5. Conclusions

Our study improves the knowledge of the regional spatial and inter-annual response of the EVI (our proxy for ANPP) to climate and how vegetation and lithology modulate this response in Mediterranean drylands. In this study, we take advantage of linear mixed-effects models (LMM), long time-series of EVI and climate data, and high-resolution vegetation and lithology maps, to evaluate the ANPP response to environmental controls at the regional scale. Along the spatial gradient, precipitation increased the EVI mean even compensating for the greater evapotranspiration of warmer sites, though with differences among substrates. The inverse relationship between the increases in MAP and in annual EVI_mean suggested the necessity of looking at the seasonal timing of the climatic and EVI trends in Mediterranean drylands. An important outcome was the effect of early-autumn climate on the EVI of the following growing season. The earlier arrival of rain after the summer drought and the cooler temperatures during early-autumn caused very strong increases in the EVI at the beginning of the growing season that may also favor the rest of the growing season. On average, the structural constraints of grasslands (shallower roots and denser canopy) for storing and using deep-soil moisture were only evident on marls, the most water-limiting substrate (Cabello, 1997; García et al., 2008), where EVI_mean was greater in scrublands. In response to the observed climate trends, grasslands showed steeper EVI_mean increases than scrublands, particularly on clays and silts, and marls. In Mediterranean drylands, where temperature and precipitation are out of phase, the overall available water for plants results from the balance between the rainfall seasonal timing and intensity, and the soil water holding capacity to carry-over soil moisture from previous seasons or years. Sites on limestones, with finer texture, deeper soils, and, hence, greater water storage capacity, showed lower dependence on current-year precipitation, and greater EVI_mean than on phyllites and schists, and marls. On the contrary, marls, with lower water storage capacity, were the most favored substrate in terms of the EVI_mean increases in response to the trends toward less water-limiting conditions.

Acknowledgments

We are sincerely thankful to the three anonymous reviewers and guest editor since their comments significantly helped us to improve the manuscript. Thanks to L. Sevilla, E. Arnau, and M. Corzofor their help processing the datasets. Financial support was given by Fondos FEDER, Junta de Andalucía (Proyectos GLOCHARID y SEGALERT P09–RNM-5048), and Ministerio de Ciencia e Innovación (Proyecto CGL2010-22314, subprograma BOS, Plan Nacional I+D+I 2010).

References

Alcaraz-Segura, D., Cabello, J., Paruelo, J.M., 2009a. Baseline characterization of major Iberian vegetation types based on the NDVI dynamics. Plant Ecology 202, 13–29.

Alcaraz-Segura, D., Cabello, J., Paruelo, J.M., Delibes, M., 2009b. Use of descriptors of ecosystem functioning for monitoring a national park network: a remote sensing approach. Environmental Management 43, 38–48.

Alcaraz-Segura, D., Liras, E., Tabik, S., Paruelo, J.M., Cabello, J., 2010. Evaluating the consistency of the 1982–1999 NDVI trends in the Iberian Peninsula across four time-series derived from the AVHRR sensor: LTDR, GIMMS, FASIR, and PAL-II. Sensors 10, 1291–1314.

Austin, A.T., Sala, O.E., 2002. Carbon and nitrogen dynamics across a natural precipitation gradient in Patagonia, Argentina. Journal of Vegetation Science 13, 351–360.

Bai, W.M., Wang, Z.W., Chen, Q.S., Zhang, W.H., Li, L.H., 2008. Spatial and temporal effects of nitrogen addition on root life span of *Leymus chinensis* in a typical steppe of Inner Mongolia. Functional Ecology 22, 583–591.

Bates, D., Sarkar, D., 2007. lme4: Linear Mixed-effects Models Using S4 Classes (R package version 0.999375-32).

Boer, M.M., Puigdefábregas, J., 2003. Predicting potential vegetation index values as a reference for the assessment and monitoring of dryland condition. International Journal of Remote Sensing 24, 1135–1141.

Bogner, C., Gaul, D., Kolb, A., Schmiedinger, I., Huwe, B., 2010. Investigating flow mechanisms in a forest soil by mixed-effects modelling. European Journal of Soil Science 61, 1079–1090.

Bolker, B.M., Brooks, M.E., Clark, C.J., Geange, S.W., Poulsen, J.R., Stevens, M.H.H., White, J.S.S., 2009. Generalized linear mixed models: a practical guide for ecology and evolution. Trends in Ecology and Evolution 24, 127–135.

Cabello, J., 1997. Factores ambientales, estructura y diversidad en comunidades de matorral de ambiente mediterráneo semiárido (Tabernas-Sierra Alhamilla-Níjar, SE. Ibérico). Tesis doctoral, Universidad de Almería.

Cabello, J., 2009. Matorrales termomediterráneos, matorrales suculentos canarios (macaronésicos) dominados por Euphorbias endémicas y nativas y tomillares semiáridos dominados por plumbagináceas y quenopodiáceas endémicas y nativas. In: Dirección General de Medio Natural y Política Forestal, Ministerio de Medio Ambiente, y Medio Rural y Marino (Eds.), Bases Ecológicas Preliminares para la Conservación de los Tipos de Hábitat de Interés Comunitario en España, VV.AA, Madrid, 170 pp.

Camacho-De Coca, F., García-Haro, F.J., Gilabert, M.A., Meliá, J., 2004. Vegetation cover seasonal changes assessment from TM imagery in a semi-arid landscape. International Journal of Remote Sensing 25, 3451–3476.

Contreras, S., Boer, M.M., Alcalá, F.J., Domingo, F., García, M., Pulido-Bosch, A., Puigdefábregas, J., 2008. An ecohydrological modelling approach for assessing

long-term recharge rates in semiarid karstic landscapes. Journal of Hydrology 351, 42–57.
Chapin, F.S., Walker, B.H., Hobbs, R.J., Hooper, D.U., Lawton, J.H., Sala, O.E., Tilman, D., 1997. Biotic control over the functioning of ecosystems. Science 277, 500–504.
Domingo, F., Sánchez, G., Moro, M.J., Brenner, A.J., Puigdefábregas, J., 1998. Measurement and modelling of rainfall interception by three semi-arid canopies. Agricultural and Forest Meteorology 91, 275–292.
Edwards, L.J., Muller, K.E., Wolfinger, R.D., Qaqish, B.F., Schabenberger, O., 2008. An R^2 statistic for fixed effects in the linear mixed model. Statistics in Medicine 27, 6137–6157.
Epstein, H.E., Paruelo, J.M., Piñeiro, G., Burke, I.C., Lauenroth, W.K., Barrett, J.E., 2005. Interactions of water and nitrogen on primary productivity across spatial and temporal scales in grassland and shrubland ecosystems. In: Porporato, A., D'Odorico, P. (Eds.), Dryland Ecohydrology. Springer-Verlag, Berlin.
Fabricante, I., Oesterheld, M., Paruelo, J.M., 2009. Annual and seasonal variation of NDVI explained by current and previous precipitation across northern Patagonia. Journal of Arid Environments 73, 745–753.
Fang, J., Piao, S., Zhou, L., He, J., Wei, F., Myneni, R.B., Tucker, C.J., Tan, K., 2005. Precipitation patterns alter growth of temperate vegetation. Geophysical Research Letters 32, 1–5.
García, M., Oyonarte, C., Villagarcía, L., Contreras, S., Domingo, F., Puigdefábregas, J., 2008. Monitoring land degradation risk using ASTER data: the non-evaporative fraction as an indicator of ecosystem function. Remote Sensing of Environment 112, 3720–3736.
Gilbert, R.O., 1987. Statistical Methods for Environmental Pollution Monitoring. John Wiley and Sons, New York, USA.
Giorgi, F., Lionello, P., 2008. Climate change projections for the Mediterranean region. Global and Planetary Change 63, 90–104.
Haase, P., Pugnaire, F.I., Clark, S.C., Incoll, L.D., 1999. Environmental control of canopy dynamics and photosynthetic rate in the evergreen tussock grass *Stipa tenacissima*. Plant Ecology 145, 327–339.
Haase, P., Pugnaire, F.I., Clark, S.C., Incoll, L.D., 2000. Photosynthetic rate and canopy development in the drought-deciduous shrub *Anthyllis cytisoides* L. Journal of Arid Environments 46, 79–91.
Hirsch, R.M., Slack, J.R., Smith, R.A., 1982. Techniques of trend analysis for monthly water quality data. Water Resources Research 18, 107–121.
Hollander, M., Wolfe, D.A., 1973. Nonparametric Statistical Methods. John Wiley and Sons, New York, USA.
Huete, A., 1988. A soil-adjusted vegetation index (SAVI). Remote Sensing of Environment 25, 295–309.
Huete, A., Liu, H., Batchily, K., Van Leeuwen, W., 1997. A comparison of vegetation indices over a global set of TM images for EOS–MODIS. Remote Sensing of Environment 59, 440–451.
Huxman, T.E., Cable, J.M., Ignace, D.D., Eilts, J.A., English, N.B., Weltzin, J., Williams, D.G., 2004. Response of net ecosystem gas exchange to a simulated precipitation pulse in a semi-arid grassland: the role of native versus non-native grasses and soil texture. Oecologia 141, 295–305.
Jobbagy, E.G., Sala, O.E., Paruelo, J.M., 2002. Patterns and controls of primary production in the Patagonian steppe: a remote sensing approach. Ecology 83, 307–319.
Kaufman, Y.J., Sendra, C., 1988. Algorithm for automatic atmospheric corrections to visible and near-IR satellite imagery. International Journal of Remote Sensing 9, 1357–1381.
Kaufman, Y.J., Tanre, D., 1992. Atmospherically resistant vegetation index (ARVI) for EOS–MODIS. Geoscience and Remote Sensing, IEEE Transactions on 30, 261–270.
Kaufman, Y.J., Tanre, D., 1996. Strategy for direct and indirect methods for correcting the aerosol effect on remote sensing: from AVHRR to EOS–MODIS. Remote Sensing of Environment 55, 65–79.
Knapp, A.K., Beier, C., Briske, D.D., Classen, A.T., Yiqi, L., Reichstein, M., Smith, M.D., Smith, S.D., Bell, J.E., Fay, P.A., Heisler, J.L., Leavitt, S.W., Sherry, R., Smith, B., Weng, E., 2008. Consequences of more extreme precipitation regimes for terrestrial ecosystems. BioScience 58, 811–821.
Knapp, A.K., Smith, M.D., 2001. Variation among biomes in temporal dynamics of aboveground primary production. Science 291, 481–484.
Lane, D.R., Coffin, D.P., Lauenroth, W.K., 1998. Effects of soil texture and precipitation on above-ground net primary productivity and vegetation structure across the central grassland region of the United States. Journal of Vegetation Science 9, 239–250.
Le Houérou, H.N., 1984. Rain use efficiency: a unifying concept in arid-land ecology. Journal of Arid Environments 7, 213–247.
Le Houérou, H.N., 1990. Global change: population, land-use and vegetation in the Mediterranean Basin by the mid-21st century. Greenhouse effect, sea level and drought. Proc. workshop, Fuerteventura, 1989, pp. 301–367.
Le Houérou, H.N., Bingham, R.L., Skerbek, W., 1988. Relationship between the variability of primary production and the variability of annual precipitation in world arid lands. Journal of Arid Environments 15, 1–18.
Liras, E., 2010. Funcionamiento ecosistémico: controles y patrones espacio-temporales en el SE Ibérico. Tesis doctoral, Universidad de Almería.
Liu, J.G., Mason, P., Hilton, F., Lee, H., 2004. Detection of rapid erosion in SE Spain: a GIS approach based on ERS SAR coherence imagery. Photogrammetric Engineering and Remote Sensing 70, 1179–1185.
Lloret, F., Lobo, A., Estevan, H., Maisongrande, P., Vayreda, J., Terradas, J., 2007. Woody plant richness and NDVI response to drought events in Catalonian (northeastern Spain) forests. Ecology 88, 2270–2279.
Miranda, J.D., Padilla, F.M., Lázaro, R., Pugnaire, F.I., 2009a. Do changes in rainfall patterns affect semiarid annual plant communities? Journal of Vegetation Science 20, 269–276.
Miranda, J.D., Padilla, F.M., Pugnaire, F.I., 2009b. Response of a Mediterranean semiarid community to changing patterns of water supply. Perspectives in Plant Ecology, Evolution and Systematics 11, 255–266.
Monteith, J.L., 1972. Solar radiation and productivity in tropical ecosystems. Journal of Applied Ecology 9, 747–766.
Noy-Meir, I., 1973. Desert ecosystems: environments and producers. Annual Review of Ecology and Systematics 4, 25–51.
Oyarzabal, M., Oyonarte, C., Giorno, A., 2008. Propuesta de un sistema de seguimiento y alerta para la gestión de espacios protegidos: el caso del Parque Natural Cabo de Gata-Níjar (Almería, España). Ecosistemas 17, 98–107.
Oyonarte, C., Alcaraz-Segura, D., Oyarzabal, M., Paruelo, J.M., Cabello, J., 2010. Sistema de apoyo a la gestión de reservas de la biosfera basado en el monitoreo de la productividad primaria: ensayo en Cabo de Gata-Níjar (Almería-España). In: Araya, P., Clüsener-Godt, M. (Eds.), Reservas de la Biosfera: Su Contribución a la Provisión de Servicios de los Ecosistemas. Experiencias Exitosas en Iberoamérica. UNESCO, Paris, pp. 119–140.
Paruelo, J.M., Oesterheld, M., di Bella, C.M., Arzadum, M., Lafontaine, J., Cahuepe, M., Rebella, C.M., 2000. A calibration to estimate primary production of subhumid rangelands form remotely sensed data. Applied Vegetation Science 3, 189–195.
Paruelo, J.M., Piñeiro, G., Oyonarte, C., Alcaraz, D., Cabello, J., Escribano, P., 2005. Temporal and spatial patterns of ecosystem functioning in protected arid areas of Southeastern Spain. Applied Vegetation Science 8, 93–102.
Pettorelli, N., Vik, J.O., Mysterud, A., Gaillard, J.M., Tucker, C.J., Stenseth, N.C., 2005. Using the satellite-derived NDVI to assess ecological responses to environmental change. Trends in Ecology and Evolution 20, 503–510.
Piñeiro, J., Bates, D., DebRoy, S., Sarkar, D., 2009. nlme: Linear and Nonlinear Mixed Effects Models (R package version 3.1-96).
Piñeiro, G., Oesterheld, M., Paruelo, J.M., 2006. Seasonal variation in aboveground production and radiation-use efficiency of temperate rangelands estimated through remote sensing. Ecosystems 9, 357–373.
Porporato, A., D'Odorico, P., Laio, F., Ridolfi, L., Rodriguez-Iturbe, I., 2002. Ecohydrology of water-controlled ecosystems. Advances in Water Resources 25, 1335–1348.
Potts, D.L., Huxman, T.E., Cable, J.M., English, N.B., Ignace, D.D., Eilts, J.A., Mason, M.J., Weltzin, J.F., Williams, D.G., 2006. Antecedent moisture and seasonal precipitation influence the response of canopy-scale carbon and water exchange to rainfall pulses in a semi-arid grassland. New Phytologist 170, 849–860.
Prieto, I., Kikvidze, Z., Pugnaire, F.I., 2010. Hydraulic lift: soil processes and transpiration in the Mediterranean leguminous shrub *Retama sphaerocarpa* (L.) Boiss. Plant and Soil 329, 447–456.
Puigdefábregas, J., Sole, A., Gutiérrez, L., Del Barrio, G., Boer, M., 1999. Scales and processes of water and sediment redistribution in drylands: results from the Rambla Honda field site in Southeast Spain. Earth Science Reviews 48, 39–70.
Russell, E.W., Wild, A., 1988. Russell's Soil Conditions and Plant Growth, eleventh ed. Longman Scientific and Technical, Harlow (UK).
Sala, O.E., Parton, W.J., Joyce, L.A., Lauenroth, W.K., 1988. Primary production of the central grassland region of the United States. Ecology 69, 40–45.
Schenk, H.J., Jackson, R.B., 2002. Rooting depths, lateral root spreads and below-ground/above-ground allometries of plants in water-limited ecosystems. Journal of Ecology 90, 480–494.
Sellers, P.J., Berry, J.A., Collatz, G.J., Field, C.B., Hall, F.G., 1992. Canopy reflectance, photosynthesis, and transpiration. III. A reanalysis using improved leaf models and a new canopy integration scheme. Remote Sensing of Environment 42, 187–216.
Sen, P.K., 1968. Estimates of the regression coefficient based on Kendall's tau. Journal of the American Statistical Association 63, 1379–1389.
Serrano-Ortiz, P., Kowalski, A.S., Domingo, F., Rey, A., Pegoraro, E., Villagarcía, L., Alados-Arboledas, L., 2007. Variations in daytime net carbon and water exchange in a montane shrubland ecosystem in southeast Spain. Photosynthetica 45, 30–35.
Verón, S.R., Paruelo, J.M., Oesterheld, M., 2006. Assessing desertification. Journal of Arid Environments 66, 751–763.
Webb, W.L., Lauenroth, W.K., Szarek, S.R., Kinerson, R.S., 1983. Primary production and abiotic controls in forests, grasslands, and desert ecosystems in the United States. Ecology 64, 134–151.
Yahdjian, L., Sala, O.E., 2006. Vegetation structure constrains primary production response to water availability in the Patagonian steppe. Ecology 87, 952–962.
Zuur, A.F., Ieno, E.I., Walker, N.J., Saveliev, A.A., Smith, G.M., 2009. Mixed Effects Models and Extensions in Ecology with R. Springer, New York.

Please cite this article in press as: Cabello, J., et al., The role of vegetation and lithology in the spatial and inter-annual response of EVI to climate in drylands of Southeastern Spain, Journal of Arid Environments (2012), doi:10.1016/j.jaridenv.2011.12.006